ARTICLES

Time Resolved Resonance Raman, Ab Initio Hartree−Fock, and Density Functional Theoretical Studies on the Transients States of Perfluoro-*p*-Benzoquinone

G. Balakrishnan, P. Mohandas, and S. Umapathy*

Department of Inorganic and Physical Chemistry, Indian Institute of Science, Bangalore-560012, India

Received: October 25, 2000; In Final Form: April 30, 2001

In recent times, perfluorinated organic compounds have been investigated extensively to understand the influence of perfluorination on structure−reactivity correlations. Here, we report the time-resolved resonance Raman (TR3), ab initio Hartree−Fock (HF), and density functional theoretical (DFT) studies on the photogenerated transient states of perfluoro-*p*-benzoquinone (Fluoranil, FA). In particular, for the triplet excited states, radical anion and ketyl radical Raman spectra have been recorded. The observed Raman excitation profiles and the decay rate constants of triplet excited states of FA satisfactorily reproduce, respectively, the absorption spectra and decay rate constants reported previously from transient absorption studies. The structure and vibrational spectra of all these intermediates of FA have been calculated using both ab initio unrestricted Hartree−Fock (UHF) and density functional (UBP86) methods with standard 6-31G(d) basis set. The assignments for all the experimentally observed resonance Raman bands are made using the calculated frequencies and the normal coordinate analysis. Potential energy distributions (PEDs) are also presented. Perfluoro effect is found to be more pronounced in the triplet excited state than in the ground state or the radical anion, whereas the effect in the ground state seems to be higher than that in the radical anion. The lowest triplet excited state of FA has been identified as the $\pi\pi^*$ state ($^3B_{3G}$) in nonpolar solvents and the $n\pi^*$ state ($^3B_{1G}$) in polar solvents. The solvent polarity appears to play a major role in the nature of the lowest triplet excited states, since these two states are very close to each other.

I. Introduction

Recently there has been considerable interest in fluorinated organic compounds due to their importance in various fields of chemistry and biology.[1−17] In many biological systems, hydrogen atom can be substituted by fluorine atom since the size of fluorine (1.2 Å) atom is very close to that of hydrogen (1.35 Å),[6] and therefore, little or no stereochemical perturbations are likely to be introduced by fluorine substitution. Further, the use of perfluoro derivatives has been realized to be an alternative for chlorofluorocarbons since chlorofluorocarbons are reported to be involved in the depletion of ozone layer in the troposphere. Thus, fluorinated organics have been studied extensively by both synthetic and physical chemists.[7,9−17]

Perfluoro derivative of *p*-benzoquinone (BQ), also known as Fluoranil (FA, see Figure 1), has been extensively studied both by spectroscopists and photochemists alike, due to its unique molecular structure and reactivity.[18−28] Eventhough its structure appears to be similar to that of BQ, fluorine substitution is reported to change the reactivity and structure.[29−35] For example, both UV−Visible and IR absorption spectral properties of FA are known to differ considerably from BQ and other related halogenated BQs, such as chloranil (CA) and bromanil (BA).[25] In general, substituents can influence the structure either by steric factors or electronic factors, such as inductive and resonance effects. The electronic factors are known to play a major role in systems having F as substituents, since the size of the F atom is relatively small and only very little steric effect is expected. The inductive effect of F induces a destabilizing effect on the organic radicals and thus results in high reactivity compared to nonfluorinated counterparts.[5]

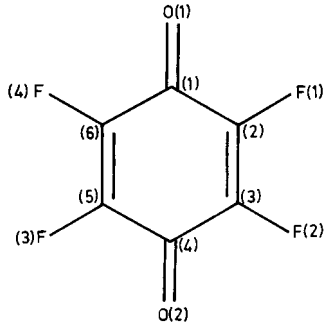

Figure 1. Molecular structure of fluoranil; numbering of atoms for geometrical structure is given in paranthesis.

The photochemical intermediates of FA, such as the triplet excited state, ketyl radical, and radical anion, have been studied using flash photolysis and pulse radiolysis techniques.[19,20] Although these experiments have provided information on the rate of the reactions and the intermediates involved, little is known about the structure of the excited state which is essential to provide an understanding of the influence of the perfluoro effect on the reactivity of the different transient states. Perfluoro effect in the ground-state structure seems to have been well

* Corresponding author. Swarna Jayanthi Fellow. Fax: 91-80-3601552. E-mail: umapathy@ipc.iisc.ernet.in.

10.1021/jp003933q CCC: $20.00
Published on Web 07/21/2001

understood.[25−28] However, there is no information available about such effects on the transient state structures. To understand the structural differences induced on the photochemical intermediates by fluorine substitution on BQ, in this paper, we report the time-resolved resonance Raman spectroscopic and computational studies on vibrational spectra and structure of the photochemical intermediates of fluoranil.

Recently, application of density functional theoretical (DFT) methods to predict the vibrational spectra of polyatomic molecules has become an important area of research due to their accuracy in reproducing the experimental data.[36−46] A variety of molecules, particularly quinones, have been extensively studied using these techniques by a number of workers.[36−39] In addition to the ground state, DFT methods are also proven to be very good in predicting the vibrational frequencies of the transient states, such as, radical anions,[40−44] radical cations,[45−47] ketyl radical,[43] and triplet excited states.[43] It is known that for the transient states of BQ,[43] such as the triplet excited state, radical anion, and ketyl radical, BP86 is an ideal method to reproduce the experimental frequencies without using any empirical scaling factor. In this paper, we have carried out similar calculations on various transients states of FA not only to aid the vibrational assignments of our experimental data but also to test the validity in using DFT methods for the perfluorinated polyatomic systems.

The objectives of the present study are as follows: (a) to identify and elucidate the structures of various photogenerated intermediates of FA, such as triplet excited states, radical anion and ketyl radical, (b) to evaluate the accuracy of prediction of vibrational frequencies and PEDs using ab initio HF and DFT methods, and (c) to understand the influence of perfluorination, i.e., the perfluoro effect, on the structure of each of the transients with respect to their BQ counterpart. The geometries, vibrational frequencies, and PEDs have been calculated in order to assign all the experimentally observed vibrational bands. Further, the Raman excitation profiles (REPs) of several modes of the triplet state have also been presented and discussed in relation to its electronic structure. The vibrational assignments of the RR spectra of all intermediates of FA have been made on the basis of normal-mode analyses.

II. Methods and Materials

A. Experimental Details. The detailed experimental setup and the procedures used for the TR3 measurements have been described previously.[47,48] The third harmonic output (355 nm) from a Q-switched Nd:YAG laser (DCR-11, Spectra Physics) was used as the photoexcitation source (pump). A tunable output (430−690 nm) from an optical parametric oscillator (OPO, MOPO 730, Spectra Physics) was used as the probe laser to observe the resonance Raman scattering. The first Stokes line (416 nm) of a homemade H_2 Raman shifter was also used as a probe wavelength. The MOPO and H_2 Raman shifter were pumped by 355 nm output from another Q-switched Nd:YAG laser (GCR-250, Spectra Physics). The laser pulses were of about 8−10 ns temporal width and energies of about 2.5 mJ for both pump and probe wavelengths. The scattered light at 90° to the laser beam was collected with a quartz lens and dispersed using a SPEX 1404 double monochromator with two gratings of 600 grooves per mm. A liquid N_2 cooled CCD (Princeton Instruments) with 576 × 384 pixels was used as the multichannel detector. The recorded Raman spectra were calibrated using known solvent bands as reference and the spectral resolution was estimated as ∼5 cm^{-1}.

B. Measurements of Raman Excitation Profiles. Raman excitation profiles (REPs) are plots of Raman excitation (probe laser) wavelength versus resonance Raman intensities normalized against a Raman band that is not resonance enhanced, such as a solvent band. These plots provide information on the origin of resonance Raman intensities and also the dynamics associated with the resonant excited state.[49,50] Qualitatively, if the vibrational modes are Franck−Condon active in the resonant electronic state, then the Raman intensities originate from the A-term resonance Raman scattering.[51] The REPs of these vibrational modes are expected to follow the absorption spectral profile of that electronic state to which the resonance excitation is being carried out. These REPs, therefore, can be used to confirm whether the resonance enhanced Raman intensity of a given vibrational mode indeed arise due to resonance excitation of that particular electronic state. Hence, we have recorded the REPs of the vibrational modes of the triplet excited state of FA by tuning the probe wavelength within the transient absorption spectral profile. The REPs of the triplet excited Raman bands were recorded at a fixed time delay of 20 ns between pump and probe pulses by varying the probe wavelength in the range of 440 to 510 nm. The IR spectra were recorded with a Bruker IFS60V spectrometer using Kbr pellet as the host material.

C. Materials. Fluoranil, KBr, and KI were obtained from Aldrich and used as received. The solvents $CHCl_3$, CH_3OH, CH_3COCH_3, and CH_3CN were of analytical grade and distilled before use. The sodium salt of FA radical anion was prepared and purified using the previously reported procedure.[52] The sample solutions were circulated through a quartz capillary using a micropump at the rate of 10 mL per minute. To avoid possible accumulation of photoproducts, samples were replaced regularly. All the experiments were performed at room temperature. In addition, the ground-state Raman spectrum was recorded at various times during the TR3 experiment. The above spectra were then subtracted from the initially recorded (at the beginning of the experiment) ground-state spectrum and were found to give a flat background. This confirms that the accumulation of photoproducts if any, are negligibly small.

D. Computational Details. The ab initio Hartree−Fock (HF) and density functional theoretical (DFT) calculations were carried out using Gaussian 94 program.[53] The gradient-corrected exchange functional of Becke, B[54] combined with 1986 gradient corrected correlation functional of Perdew, P86[55] has been employed for the DFT (represented as BP86) calculations. The ground state (i.e., S_0 state of FA) calculations were performed using both Hartree−Fock (RHF) and density functional (DF) formalisms employing restricted closed shell wave functions.[54−58] For the case of transient states of FA, such as radical anion, ketyl radical, and triplet excited states, Hartee−Fock (UHF) and DFT (UBP86) formalisms employing unrestricted open shell wave functions have been adopted. Both HF and DFT calculations were performed using the standard double-ζ plus polarization (DZ), 6-31G(d) basis set. In all the cases, a complete geometry optimization was carried out using Berny's optimization algorithm.[59] The ground state (S_0), triplet excited states (T_1 and T_2), and radical anion ($FA^{\bullet -}$) have been optimized with D_{2h} symmetry, whereas for the ketyl radical ($FAH^{\bullet}$), C_s symmetry has been adopted. The spin contamination due to the use of unrestricted wave functions was found to be minor. For example, the expectation value, $\langle S^2 \rangle$, obtained from the UBP86/6-31G(d) calculations were found to be 2.004 for T_1, 2.006 for T_2, and 0.753 for the radical anion, and these values are very close to the expected values of 2 for the triplet excited state and 0.75 for the doublet radical anion. In the case of UHF/6-31G(d) method, the calculated $\langle S^2 \rangle$ values, such as 2.113 for T_1, 2.121 for T_2, and 0.865 for the radical anion, indicates that

SCHEME 1

$$FA \xrightarrow{h\nu} {}^1FA^* \longrightarrow {}^3FA^* \quad \text{.....(1)}$$

$${}^1FA^* \longrightarrow FA \quad \text{.....(2)}$$

$${}^3FA^* \longrightarrow FA \quad \text{.....(3)}$$

$${}^1FA^* + \text{Solvent} \longrightarrow {}^1(FA \cdots \text{Solvent})^* \quad \text{.....(4)}$$

$${}^1(FA \cdots \text{Solvent})^* \longrightarrow (FA^{\cdot -} \cdots \text{Solvent}^{\cdot +}) \quad \text{.....(5)}$$

$${}^1FA^* + \text{Solvent / DH} \longrightarrow FAH^{\cdot} \longrightarrow FA^{\cdot -} \quad \text{.....(6)}$$

$${}^3FA^* + \text{Solvent} \longrightarrow {}^3(FA \cdots \text{Solvent})^* \quad \text{.....(7)}$$

$${}^3(FA \cdots \text{Solvent})^* \longrightarrow (FA^{\cdot -} \cdots \text{Solvent}^{\cdot +}) \quad \text{.....(8)}$$

$${}^3FA^* + \text{Solvent / DH} \longrightarrow FAH^{\cdot} \longrightarrow FA^{\cdot -} \quad \text{.....(9)}$$

$${}^3FA^* + \text{Solvent / DH} \longrightarrow FAH^{\cdot} \longrightarrow FA^{\cdot -} \quad \text{.....(10)}$$

the spin contamination due to use of open shell wave function in UHF methods is higher compared to that using the UBP86 method. However, it has been observed that such spin contamination does not have significant influence on either the calculated structural parameters or the vibrational frequencies.[40−47] The bond orders were calculated at the optimized geometries using natural bond order (NBO) analysis. Vibrational frequencies and normal modes were also calculated at the optimized geometries using analytical derivative techniques. Assignment of the vibrational frequencies were made by performing a normal-mode analysis using MOLVIB[60] and NMODES[43] programs. The vibrational frequencies obtained using RHF and UHF methods are uniformly scaled by an empirical factor of 0.89, as recommended by Hehre et al.,[61] whereas those obtained using BP86 method are presented without scaling. All the HF and DFT calculations were performed on IBM-RS6000 computers. Because of the limited computational resources, the frequency calculations for the ketyl radical were performed using 6-31G basis set. The exchange and correlation functionals and the 6-31G and 6-31G(d) basis sets were used as contained within the program.

III. Results and Discussion

A. Experimental. Photochemistry of fluoranil involves various transient intermediates such as singlet and triplet excited states, excited state complexes, ketyl radicals, and radical anions. Scheme 1 shows some of the possible processes induced following the photoexcitation of FA. Photoexcitation of FA using a 355 nm laser pulse leads to the formation of triplet excited state through intersystem crossing from the singlet state in the picosecond time scale with a quantum yield of nearly unity.[20,62]

The available electronic absorption spectra of FA intermediates, such as radical anion, ketyl radical, and triplet excited states, are shown along with their ground-state spectra (300−420 nm region) in Figure 2. The ground state has a band around 330 nm. The 355 nm laser pulse, which is in resonance with the 330 nm band of the ground state, has been used as the pump laser to initiate the photochemistry in various solvents. The radical anion has absorption maxima at 410 and 435 nm with molar extinction coefficients of 13 000 and 7600 M^{-1} cm^{-1}, respectively.[19] The ketyl radical has absorption maxima at 310 and 420 nm with the molar extinction coefficients of 11 000 and 5600 M^{-1} cm^{-1}, respectively.[19] The probe laser pulse of wavelength 416 nm has been used to observe the resonance Raman scattering of the radical anion and ketyl radical since both have significant absorption at this wavelength. The pK_a value is reported to be −1.[19] Therefore, under neutral pH, as in the case of the present experimental conditions, the ketyl radical is expected to deprotonate to form the radical anion. The triplet−

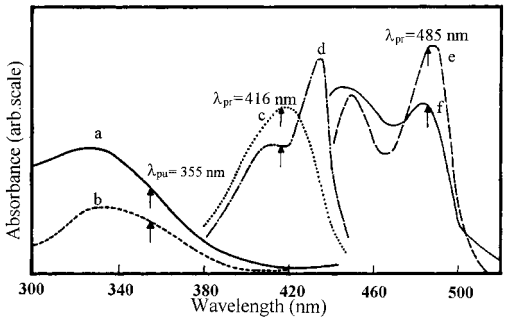

Figure 2. UV-visible absorption spectrum of fluoranil in (a) CH_3CN, (b) $CHCl_3$, (c) ketyl radical in water, (d) radical anion in water, (e) triplet excited state in $CHCl_3$, and (f) triplet excited state in CH_3CN. (panels c and d were adapted from ref 19, and e and f were adapted from ref 20).

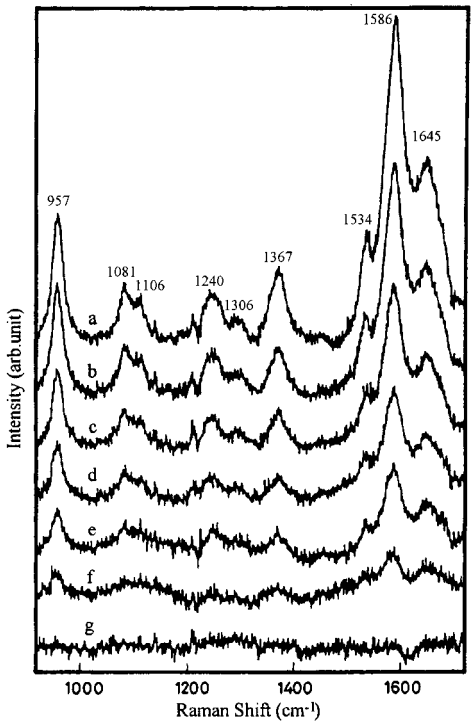

Figure 3. Time-resolved resonance Raman spectra of triplet fluoranil in $CHCl_3$, at various time delays (λ_{pump} 355 nm, λ_{probe} 485 nm): (a) 20, (b) 50, (c) 100, (d) 150, (e) 200, (f) 300, and (g) 500 ns.

triplet absorption spectrum of FA has bands at ∼450 and ∼485 nm in various solvents. The absorption spectra of triplet FA in CH_3CN and $CHCl_3$ are also given in Figure 2. Since the triplet excited state of FA absorbs at ∼485 nm with ϵ^T_{max} = 7200 M^{-1} cm^{-1} in $CHCl_3$,[20] the Raman scattering of the triplet excited state for the 485 nm excitation is expected to be resonance-enhanced. Therefore, to record the TR3 spectra of the triplet excited state of FA, 485 nm has been used as the probe wavelength. The pump and probe wavelengths employed in this study are indicated with arrows in the absorption spectrum as shown in Figure 2.

1. TR3 Spectra of Fluoranil in Chloroform. The TR3 spectra of FA in chloroform obtained using 355 nm as pump and 485 nm as probe wavelengths are shown in Figure 3. The region between 900 and 1700 cm^{-1} only is shown in the figure for simplicity, and also, the structural changes upon photoexcitation are expected to be reflected mainly in this region. The bands due to the ground-state FA and the solvent bands have been subtracted. The spectra show several bands with varying intensities which are found to decay in a few hundred

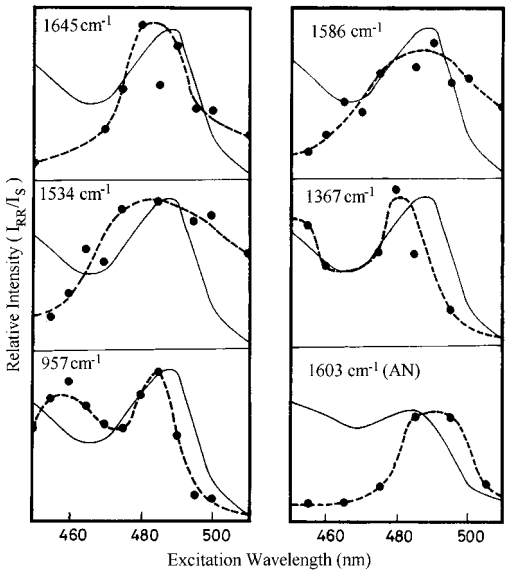

Figure 4. REPs of triplet fluoranil in $CHCl_3$ and in CH_3CN (indicated as AN) [solid line, triplet−triplet absorption spectra fluoranil; dashed line with dots, Raman excitation of the triplet fluoranil bands].

nanoseconds. The transient Raman bands observed in this region are at 957, 1081, 1106, 1240, 1306, 1367, 1534, 1586, and 1645 cm^{-1}. On the low-frequency side (below 900 cm^{-1}), four bands are observed at 270, 418, 539, and 834 cm^{-1}. The kinetic analyses on various bands have been carried out by a procedure reported earlier.[48] Here the solvent band at 1218 cm^{-1} was used to normalize the spectra obtained at different delay times. The REPs of the intense resonance Raman bands of the triplet FA in chloroform are shown in Figure 4, along with the corresponding transient absorption spectrum reported in the literature.[20] Each point in the REPs was obtained from the TR3 spectra obtained at 20 ns delay time between pump and probe lasers at all probe wavelengths. From Figure 4, it is apparent that all the modes are found to reproduce the long wavelength side of the triplet absorption spectrum reasonably well except for the bands at 1534 and 1586 cm^{-1}. The reason for the discrepancy of these two bands can be attributed to the considerable overlap of these bands along with the 1645 cm^{-1} band, resulting in poor accuracy in determining the intensities. The observed TR3 spectrum is identified as the triplet excited state of FA for the following reasons: (a) kinetic analyses of all the transient bands result in nearly the same pseudo-first-order rate constant (k^T, in the presence of air) with an average value of 4.92×10^6 s^{-1}, which is comparable to the reported value (0.38×10^6 s^{-1}) for the triplet state of FA from transient absorption studies;[20] (b) the probe wavelength of 485 nm is in resonance with the $T_n \leftarrow T_1$ absorption of the triplet state of FA in chloroform,[20] and therefore, the intense bands observed must originate due to resonance enhancement of the triplet excited state; and (c) the REPs reproduce the $T_n \leftarrow T_1$ absorption spectrum reasonably well.

Figure 5 shows the TR3 spectra of FA in chloroform using 355 nm as pump and 416 nm as probe wavelengths. Similar to the previous experiment, here again, the solvent band at 1218 cm^{-1} has been used for normalization and the ground state and the solvent bands have been subtracted. These spectra contain a strong band at 1561 cm^{-1} and three weak bands at 1645, 1418, and 1348 cm^{-1}. The transient intermediate corresponding to the above spectra is identified as the ketyl radical for the following reasons. As shown in Scheme 1, it is likely that 355 nm excitation of FA leads to the formation of ketyl radical from its triplet excited state through hydrogen abstraction from the

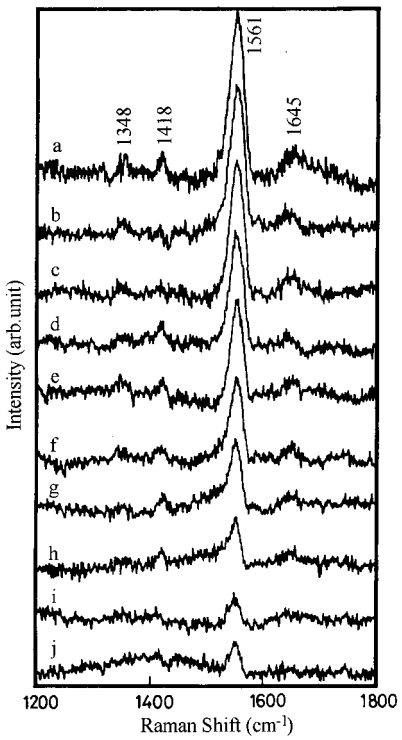

Figure 5. Time-resolved resonance Raman spectra of triplet fluoranil in $CHCl_3$, at various time delays (λ_{pump} 355 nm, λ_{probe} 416 nm): (a) 20 ns, (b) 150 ns, (c) 250 ns, (d) 900 ns, (e) 1.5 μs, (f) 3.0 μs, (g) 5.0 μs, (h) 11.0 μs, (i) 18.0 μs, and (j) 23.0 μs.

solvent, since such reactions have been reported in the literature for bromanil.[63] However, the possibility of observing the radical anion resonance Raman bands should also be considered, since both the ketyl radical and radical anion have significant absorption at the probe wavelength of 416 nm. In the earlier report on FA in 2-propanol, it is known that with time, the ketyl radical dissociates to form radical anion.[64] Therefore, the resonance Raman spectra of both species have been individually identified with the same probe wavelength. But the spectral changes associated with timein these two solvents (i.e., in $CHCl_3$ and 2-propanol) were found to be considerably different. For example, in 2-propanol, two sets of bands with different decay rate constants were obtained,[63] whereas in $CHCl_3$, all the bands are found to decay with same rate constant. The radical anion bands observed in 2-propanol have not been observed in $CHCl_3$, whereas the ketyl radical bands observed in 2-propanol and in $CHCl_3$ are similar in terms of band position and intensity. Thus, we assign the spectra observed in $CHCl_3$ using 416 nm as the probe wavelength to the ketyl radical of FA. It is possible that because of the relatively low polarity of $CHCl_3$, the radical anion may not be effectively stabilized as in 2-propanol, and only the ketyl radical may be present in the $CHCl_3$ solution.

2. TR3 Spectra of Fluoranil in Acetonitrile. The TR3 spectra (900−1700 cm^{-1} region) of FA in acetonitrile using 355 nm as pump and 485 nm as probe wavelengths are shown in Figure 6. The solvent band at 1375 cm^{-1} has been to used to normalize the spectra at different times, and the bands of FA ground state and solvents have been subtracted. The transient spectra show an intense band at 1603 cm^{-1}. The other bands observed in this region are at 958, 1087, 1240, 1299, and 1543 cm^{-1}. The kinetic analyses of the intense bands give nearly the same pseudo first-order rate constant as that in $CHCl_3$ (k^T, in the presence of air) with value of 3.85×10^6 s^{-1}, which is comparable to the reported value[20] for triplet FA from flash photolysis studies. Hence, the observed TR3 spectrum is identified as that corre-

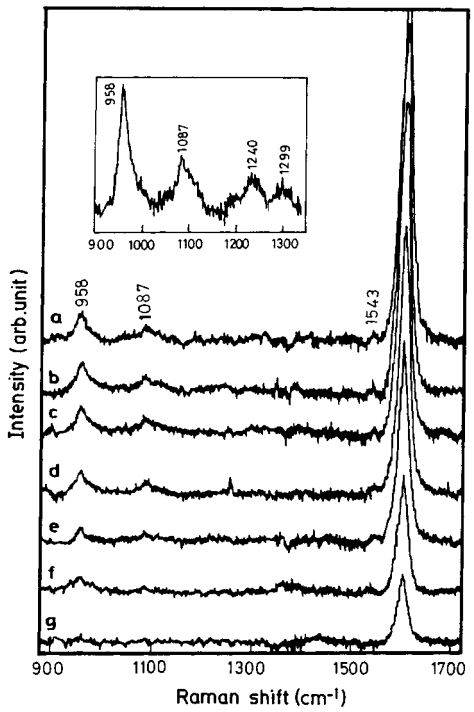

Figure 6. Time-resolved resonance Raman spectra of triplet fluoranil in CH_3CN, at various time delays (λ_{pump} 355 nm, λ_{probe} 485 nm): (a) 10, (b) 20, (c) 40, (d) 80, (e) 150, (f) 300, and (g) 500 ns. Inset: Expanded vertically for the region 800−1400 cm^{-1}.

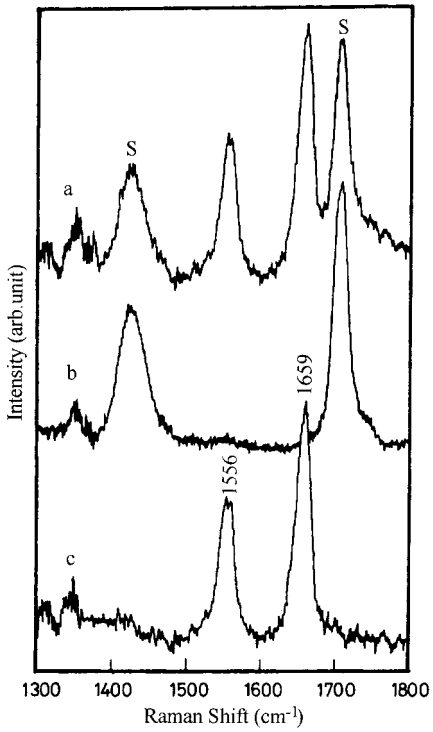

Figure 7. Resonance Raman Spectra recorded using 441 as probe wavelength (a) fluoranil + KI in acetone (solvent bands are indicated as **S**), (b) acetone, and (c) a − b, the radical anion of fluoranil.

sponding to the triplet excited state of FA. This is also supported by the resonance enhancement observed for 485 nm probe wavelength ($T_n \leftarrow T_1$ absorption). The triplet state of FA in acetonitrile has only one intense resonance Raman band at 1603 cm^{-1}, and its REP (denoted as AN in Figure 4) is included in Figure 4, along with the corresponding transient absorption spectrum reported in the literature.[20] This band is very similar to the REPs of all the bands that are observed in $CHCl_3$ and found to reproduce the long wavelength side of the triplet absorption spectrum reasonably well. The transient bands on the low-frequency side (below 900 cm^{-1}) were found to be very weak compared to those observed in chloroform solution. These bands are observed at 270, 419, and 543 cm^{-1}.

3. Radical Anion Resonance Raman Spectrum of Fluoranil in Acetone. The resonance Raman spectrum of FA radical anion obtained using 441 nm as the excitation wavelength is shown in Figure 7. The radical anion was prepared by means of chemical reduction by mixing equimolar solutions of FA in acetone and KI in acetone in the Raman cell. The radical anion so generated is stable enough to record its RR spectrum (upto 2−5 min). The radical anion spectrum shown in Figure 7c is the difference spectrum obtained by subtracting the FA/acetone solution spectrum which is obtained before reduction (Figure 7b) from the spectrum obtained after the reduction (Figure 7a). As seen from Figure 7c, the radical anion has only two strong bands at 1556 and 1659 cm^{-1}. The similarity of this spectrum to the reported radical anion resonance Raman spectrum from a pulse radiolysis study[21] confirms that the above spectrum is due to radical anion.

4. FTIR Spectrum of Fluoranil Radical Anion. The IR spectra of neutral FA and its radical anion salt are shown in Figure 8a and 8b, respectively. The disappearance of all the bands corresponding to the neutral FA in the radical anion salt spectrum (Figure 8b) indicates that no neutral species is contributing to this spectrum. Several bands, such as those at

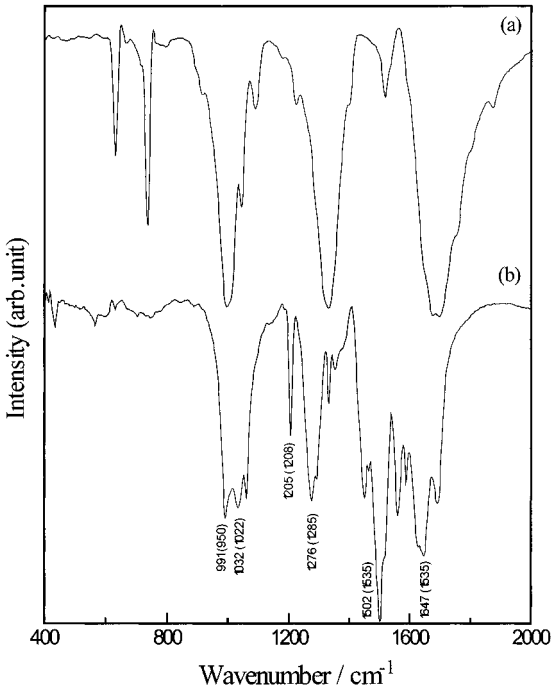

Figure 8. FTIR spectra of fluoranil (KBr pellet method): (a) neutral molecule and (b) sodium salt of the radical anion (bands labeled corresponding to the fundamental modes and values in parentheses are calculated using UBP86 method).

1691, 1647, 1628, 1587, 1560, 1520, 1502, 1464, 1450, 1354, 1333, 1292, 1276, 1205, 1186, 1061, 1032, 991, 628, 565, and 432 cm^{-1}, were observed in the region of 400 to 2000 cm^{-1}. All these bands were assigned to fundamentals, overtones, and numbers of combination bands. The fundamental bands are labeled in Figure 8b and the corresponding calculated (from UBP86 method) values are given in parentheses.

TABLE 1: Optimized Structural Parameters for Fluoranil (S_0), Its Triplet States (T_1 and T_2) and Radical Anion ($FA^{\bullet-}$)

structural[a] parameter	FA (S_o)			FA (T_1)		FA (T_2)		$FA^{\bullet-}$	
	RHF	BP86	exp.[b,c]	UHF	BP86	UHF	BP86	UHF	BP86
C═C	1.318	1.359	1.339 (1.339)	1.411	1.430	1.336	1.373	1.348	1.380
C═O	1.183	1.230	1.215 (1.211)	1.219	1.249	1.241	1.281	1.236	1.268
C−C	1.490	1.494	1.475 (1.489)	1.432	1.461	1.438	1.450	1.439	1.461
C−F	1.306	1.335	1.323 (1.323)	1.293	1.327	1.311	1.341	1.333	1.365
C═C−C	121.9	121.8	121.8 (121.6)	124.8	124.6	121.2	121.5	123.5	123.6
C−C═O	121.9	121.8	121.8 (121.6)	124.8	124.6	121.2	121.5	123.5	123.6
C−C−C	116.3	116.4	116.9 (116.8)	110.4	110.7	117.5	117.1	113.0	112.8
C−C−F	115.4	115.9	116.1 (116.1)	118.4	117.8	116.6	116.9	117.2	117.0

[a] Bond lengths in Å and bond angles in deg; for definition of parameters, see Figure 1. [b] X-ray diffraction values from ref 23. [c] Electron diffraction values in parentheses from ref 22.

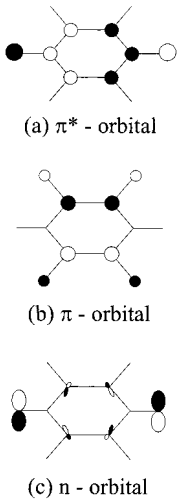

Figure 9. Molecular obitals of Fluoranil: (a) π^* orbital, (b) π orbital, and (c) n orbital (see the text for detailed description).

B. Computational. Before proceeding to the discussion on the calculated structures of various intermediates, first we consider the nature of triplet excited states of FA. The energy separation between the lowest ($\pi\pi^*$) and the next-nearest ($n\pi^*$) triplet excited states of FA was reported to be only about 1000 cm^{-1} in cyclohexane.[25] The TR3 spectra of triplet FA in polar (CH_3CN) and nonpolar ($CHCl_3$) solvents are observed to be dissimilar (see Figures 6 and 3). It is possible therefore, that the triplet state observed in polar solvents is different from that in nonpolar solvents or that it has mixed character of the two states ($\pi\pi^*$ and $n\pi^*$). In polar solvents, the lowest triplet excited state is likely to be one of these two triplet excited states. Further, it is also possible that the lowest excited triplet state might have mixed characters of these two states. Thus, to gain more insight into the structure and nature of the triplet excited states of FA, we have considered these two triplet excited states as low-lying $\pi\pi^*$ and $n\pi^*$ states of FA.

Complete optimization of the triplet excited state of FA with D_{2h} symmetry at the initial guess resulted in a stable structure with transfer of electron from a π orbital (b_{1g}) character to an antibonding π^* orbital (b_{2g}), which corresponds to the $\pi\pi^*$ excitation. The other triplet excited state with $n\pi^*$ configuration is obtained by exciting an electron from an n orbital (b_{3g}), which is localized on the oxygen atom to a π^* orbital (b_{2g}). The molecular orbitals of FA which are pertinent to the present discussion are shown in Figure 9. The MO with b_{1g} symmetry belongs to C═C bonding π-orbitals, and the MO with b_{2g} symmetry corresponds to antibonding character with respect to C═C and C═O bond and bonding character with respect to C−C bond. There are two possible n orbitals for consideration due to symmetric (n^+) and antisymmetric (n^-) combinations of lone pair (P_z) orbitals on oxygen atoms,[18] but only the excitation of n^- with b_{3g} symmetry results in stable structure, and therefore, the b_{3g} orbital is also shown in Figure 9. For this excitation, the computational results present another stable structure again with D_{2h} symmetry but different electronic state, i.e., $n\pi^*$. The energy difference was calculated to be 1148 cm^{-1} (3.3 kcal mol^{-1}, obtained from the UBP86 method) between the two possible triplet excited states, which is close to the previously reported value.[25] We refer to the lowest triplet excited state with $\pi\pi^*$ character as T_1 and the next state with $n\pi^*$ character as T_2 state. Both T_1 and T_2 states do not correspond to any transition state since the vibrational frequency calculations do not give any negative (imaginary) frequencies as expected for a transition state.

C. Geometrical Structure. The optimized structural parameters for the FA ground state (S_0) and its transient states are listed in Table 1. The available X-ray and electron diffraction values for the ground state[22,23] are also included in the table for comparison. The numbering of the atoms adopted in the calculations are shown in Figure 1. In all the cases, C_5-C_6 and C_2-C_3 bonds are represented as C═C throughout the discussion in order to distinguish these bonds from the other set of C−C bonds (C_1-C_2, C_3-C_4, C_4-C_5, and C_1-C_6). Because of the different molecular symmetry and the different numbering scheme, the ketyl radical will be discussed separately for the sake of convenience. The bond order values are also expected to yield further insight into the molecular structure, and therefore, the calculated bond orders for various intermediate states of FA, including the ground state, are shown in Figure 10.

1. Ground State S_0. As seen from Table 1, the C═C, C═O and C−F bond distances obtained at the Hartree−Fock (RHF) level are underestimated, whereas those obtained using BP86 method are overestimated in comparison with the corresponding experimental (X-ray and electron diffraction) values. The C−C bond distances of 1.490 Å (RHF) and 1.494 Å (BP86) are found to be close to the experimental (from electron diffraction) value of 1.489 Å. However, X-ray diffraction indicates a shorter C−C bond length (1.475 Å). Bond angles calculated using both methods are in good agreement with the corresponding experimental values. The calculated bond order values (see Figure 10) of 1.606 for C═C and 1.021 for C−C suggest that the benzene ring contains single and partial double bonds with a typical quinonoid structure. Here, we concentrate mainly on the transient states of FA, since Boesch and Wheeler[36] have already reported the ground state properties of FA reasonably well.

2. Triplet State T_1. Although the absolute values of the bond distances calculated using UHF and UBP86 methods show large differences, the trends in the variation of the structural parameters for the triplet excited state compared to those for the ground state are found to be similar for both methods. The C═C bond

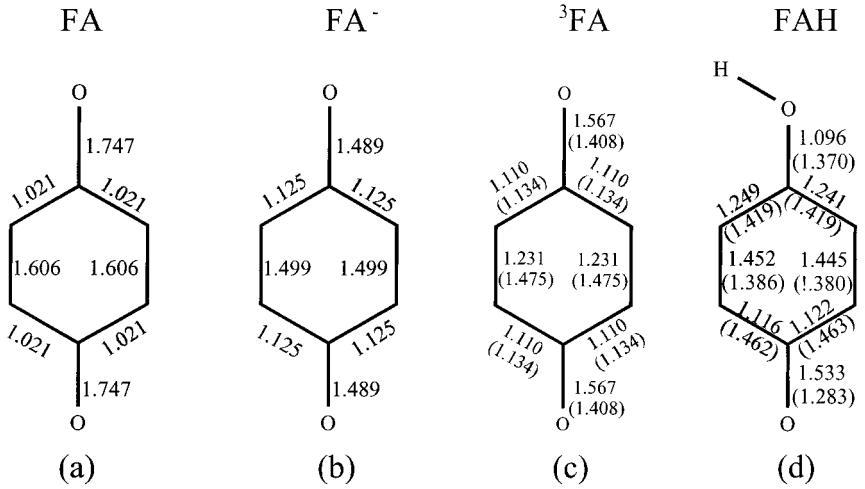

Figure 10. Calculated bond orders of fluoranil in the (a) ground state, (b) radical anion, (c) triplet (T_1) excited state (values in parentheses correspond to the T_2 state), and (d) ketyl radical. (The calculated C−C and C−O bond lengths (in Å) of fluoranil ketyl radical are given in parentheses.)

distances for the triplet show a large increase compared to those for the ground state, and the values indicate only a partial double bond character. From Figure 10, we can see that there is a reduction in the bond order from the ground state (1.606) to the triplet excited state (1.231). The C═O bonds also show significant lengthening on $\pi\pi^*$ excitation to the triplet excited state. However, the increase in the C═O bond distances is found to be much smaller than that seen for C═C bonds. Similarly, the corresponding bond order is also found to be reduced for this triplet state with respect to ground state, but the magnitude of such reduction is small compared to the C═C bond order. On the other hand, the C−C bonds are shortened significantly (0.058 and 0.033 Å, respectively, for UHF and BP86 methods) in the triplet state, as supported by the calculated increase in bond order value. The C−F bonds show only small variations compared to the ground state. These variations in the bond distances of T_1 show that in the $\pi\pi^*$ triplet excited state, the molecule is elongated along the C═O axis and compressed along the direction perpendicular to that. This is further evidenced by the increase of C═C−C and C−C═O bond angles and decrease of C−C−C bond angle. The structural changes involved here can be explained by considering the calculated electronic structure for the triplet state. As discussed earlier, the present calculation shows that T_1 of FA with an electronic state of $^3B_{3g}$ corresponds to a $\pi \rightarrow \pi^*$ excitation of an electron from the b_{1g} orbital (HOMO of FA) to the antibonding π^* orbital b_{2g} (LUMO of FA), thus giving an electronic configuration of $...(b_{1g})^1 (b_{2g})^1$. The population of the b_{2g} (see Figure 9) orbital, which is antibonding with respect to C═C and C═O bonds and bonding with respect to C−C bonds, is consistent with the predicted changes in bond lengths. It is interesting to note that, in the case of BQ, the C═O bonds were found to elongate more compared to the C═C bonds in the lowest excited triplet state. This is not surprising, since the BQ triplet (T_1) is $n\pi^*$ in nature[43,65,66] whereas the T_1 state of FA is $\pi\pi^*$ in nature.

3. Triplet State T_2. A second triplet state (T_2) was obtained by exciting a lone pair electron from an n orbital (instead from π orbital as discussed for T_1) to the π^* orbital. The calculated geometrical parameters of T_2 (Table 1) show that its structure is different from that of the T_1 state. For example, in contrast to T_1, the C═O bond length of T_2 show an increase larger than the C═C bond distances. This is consistent with the calculated electronic state of T_2, with electronic configuration of $...(b_{3g})^1 (b_{2g})^1$, corresponding to the state with $^3B_{1g}$ symmetry, which is of $n\pi^*$ character. Another interesting observation is the change in the C−C−C angle relative to the ground state and the T_1 state. Almost very similar values for the ground and T_2 states are obtained as opposed to the T_1 state, suggesting that the $n\pi^*$ excitation has very little effect on the benzene ring part of the molecule. Hence, the structural changes associated with this excitation is very similar to T_1 state of BQ since the lowest triplet excited state of BQ is also $n\pi^*$ state.[43,66]

4. Radical Anion. The calculated electronic structure of the radical anion shows that it corresponds to a $^2B_{2g}$ state with a singly occupied b_{2g} antibonding π^* orbital. The variation in the structural parameters of this radical anion as compared to the ground state are found to be very similar to those observed for BQ.[43] This is because of the identical nature of the electronic states involved in both cases. As seen from Table 1, in comparison with the ground state, the C═C and C═O bonds of the radical anion are elongated, whereas the C−C bonds are shortened. These significant changes in the bond distances of the radical anion show that the molecule is elongated along the C═O axis and is compressed in the direction perpendicular to that. The calculated bond angles agree well with this observation.

5. Ketyl Radical. The important bond distances calculated using the UBP86 method are given (values in parentheses) in Figure 10d. The C_5-C_6 and C_2-C_3 bond distances are found to be 1.386 and 1.380 Å, respectively, with the corresponding bond orders of 1.445 and 1.452. This shows that these bonds are compared to the C═C distances in the ground state, suggesting partial double bond character. The C_4-O_2 bond distance is calculated to be 1.283 Å. The corresponding bond order is 1.533 (see Figure 10d). This bond also shows elongation (by 0.023 Å) compared to the C═O bonds in ground-state FA. The other C−O distance of 1.351 Å suggests that it is more of a single bond. The bond distance and bond order values for the remaining four C−C bonds show that C_1-C_6 and C_1-C_2 are shortened to a greater extent than the other two C_3-C_4 and C_4-C_5 with respect to the ground state.

D. Vibrational Frequencies and Assignments. *1. Ground State S_0.* The structure of FA in its ground state has been reported by both experimental and theoretical studies.[22−25,36] Electron diffraction[22] and X-ray diffraction[23] structural studies reveal that the F and O atoms are arranged alternatively slightly away from the mean plane defined by the ring carbon atoms. However, it has been reported that it is reasonable to assume D_{2h} symmetry for FA in the ground state.[24,36]

TABLE 2: Vibrational Frequencies,[a] PEDs, and Approximate Descriptions for the In-Plane Normal Modes of Fluoranil Ground State

		frequency (cm^{-1})				
sym.	species	RHF[b]	UBP86	exp.[c]	PED (%)[d]	approximate description
a_g	ν_1	1822	1701	1700	C═O (48), C═C (34)	C═O stretch
	ν_2	1765	1678		C═C (46), C═O (38)	C═C stretch
	ν_3	1235	1238	1240	C−F (64), C−C (21)	C−F stretch
	ν_4	524	528	540	C−C (56), C−F (20)	ring breath
	ν_5	402	408	420	δCCC (76)	ring bend
	ν_6	258	251	271	δCCF (79)	C−F bend
b_{3g}	ν_{23}	1367	1347	1378	C−C (46), C−F (32)	C−C stretch
	ν_{24}	1097	1094	1107	C−F (54), C−C (28)	C−F stretch
	ν_{25}	780	776		δCCF (51), δCCO (28)	C−F + C═O bend
	ν_{26}	395	385	420	δCCC (62), δCCF (20)	ring bend
	ν_{27}	277	265	290	δCCF (31), δCCO (43)	C−F + C═O bend
	ν_{10}					C═O stretch
b_{1u}	ν_{11}	1809	1690	1700	C═O (88)	C−F stretch
	ν_{12}	1317	1319	1329	C−F (57), C−C (19), δCCC (17)	C−C stretch
	ν_{13}	1017	1019	1043	C−C (45), C−F (21), δCCF(20)	ring bend
	ν_{14}	598	597	630	δCCC (66), C−F (19)	C−F bend
	ν_{18}	293	295	310	δCCF (77)	C═C stretch
b_{2u}	ν_{19}	1727	1640	1669	C═C (89)	C−C stretch
	ν_{20}	1339	1305	1315	C−C (69), C−F (23)	C−F stretch
	ν_{21}	978	986	995	C−F (51), C−C (17), δCCO (19)	C═O bend
	ν_{22}	359	348	369	δCCO (61), δCCF (22)	C−F bend
		281	271	295	δCCF (82)	

[a] δ bending. [b] RHF values are uniformly scaled by 0.89. [c] Experimental values are from ref 24. [d] Calculated using BP86/6-31G(d) force field.

The symmetries, frequencies (RHF, BP86 and experimental), potential energy distributions (PEDs), and approximate descriptions for the in-plane normal modes of FA are listed in Table 2. The experimental frequencies are those reported by Girlando and Pecile.[24] The results of BP86 calculation give frequencies which are in excellent agreement with the experimental values. The PEDs calculated for the two totally symmetric (a_g) normal modes at 1701 and 1678 cm^{-1} show significant mixing of C═O and C═C stretching local modes. For the 1701 cm^{-1} mode, C═O stretching contribution is more, whereas in the case of 1678 cm^{-1} mode, C═C stretching is dominant. Hence, these modes are assigned respectively to C═O and C═C stretching fundamentals. The assignments of all the in-plane normal modes based on the calculated PEDs are summarized in the table. These assignments are consistent with those reported in an earlier study using empirical normal coordinate calculations.[24]

2. Triplet State T_1. For the triplet excited states, the experimentally observed frequencies corresponding to ^{3}FA in nonpolar solvent, such as $CHCl_3$, is compared with the calculated spectra in the T_1 state, and the experimental data in polar solvents like in alcohols and in acetonitrile are compared with the calculated spectrum corresponding to T_2 state. This procedure is followed since, as discussed earlier, the T_1 and T_2 states correspond to $\pi\pi^*$ and $n\pi^*$ states, respectively. Therefore, in nonpolar solvents such as CCl_4 and $CHCl_3$, the lowest triplet excited state is likely to be $\pi\pi^*$ state.

The symmetries, frequencies, PEDs, and approximate descriptions for the in-plane normal modes of FA triplet (T_1) obtained using UHF and UBP86 methods along with experimental frequencies are listed in Table 3. As seen from the table, the frequencies of a_g and b_{3g} modes obtained at the UHF level (values are scaled by 0.89) are comparable to those obtained using the UBP86 method. However, there are large discrepancies seen for b_{1u} and b_{2u} normal modes. For e.g., the C═C stretching frequency, i.e., (b_{2u}) calculated using the two methods, are 1707 (UHF) and 1313 cm^{-1} (UBP86). Such differences are also seen for modes such as C−F stretch (b_{1u}), C−C stretch (b_{2u}), and C−F stretch (b_{2u}). It is not possible at present to comment on the reliability of these methods in predicting the vibrational frequencies of these ungerade modes since no experimental frequencies are available for the triplet excited states. The resonance Raman spectrum of FA triplet species in chloroform contains bands at 270, 418, 539, 834, 957, 1081, 1106, 1240, 1306, 1367, 1534, 1586, and 1645 cm^{-1}. Of these, the most intense band observed at 1586 cm^{-1} can be assigned either to the totally symmetric (a_g) C═C or C═O stretching fundamental. However, the calculated results in Table 3 indicate that the high-frequency modes at 1611 (UHF) and 1610 cm^{-1} (UBP86) correspond to C═O stretching mode, whereas the calculated frequencies at 1535 (UHF) and 1511 cm^{-1} (UBP86) correspond to C═C stretch. On the basis of the calculated results and also due to the fact that the excitation is $\pi-\pi^*$ in nature, we assign the band at 1586 cm^{-1} to the C═C stretch and the mode at 1534 cm^{-1} to C═O stretch. From an intensity point of view, we note that for BQ and related compounds,[64−66] the RR intensities for the C═C stretching modes are generally larger than those for C═O stretching modes. Hence, the relative intensity considerations also seem to suggest the assignment of the band at 1586 cm^{-1} to the C═C stretching fundamental which is the most intense band. The RR bands observed at 1306 cm^{-1} can be assigned to the C−F stretching (a_g) fundamental. The bands observed at 539, 418, and 270 cm^{-1} can be assigned to the a_g fundamentals of ring breath, ring bend, and C−F bend, respectively. As seen from the table, the calculated vibrational frequencies using both UHF and UBP86 methods are in reasonable agreement with the experimental values.

The remaining bands observed in $CHCl_3$ at 1645, 1367, 1240, 1106, 1081, 957, and 834 cm^{-1} are assigned as overtones and combination bands. The bands observed at 834, 1240, and 1645 cm^{-1} are ascribed to the first, second, and third overtones of C−C−C bend (2,3 & 4 × 418 cm^{-1}), respectively. The bands at 1367 and 1106 are assigned to the combinations of the first overtone of C−C−C bend and ring breathing (2 × 418 + 539 cm^{-1}) and the first overtone of C−C−C bend and C−F bend (2 × 418 + 270 cm^{-1}), respectively. The band observed at 1081 cm^{-1} is assigned to the first overtone of ring breathing (2 × 539 cm^{-1}) mode. The band at 957 cm^{-1} is assigned to another

TABLE 3: Vibrational Frequencies,[a] PEDs, and Approximate Descriptions for the In-plane normal Modes of Fluoranil Triplet (T_1) State

		frequency (cm^{-1})				
sym.	species	UHF[b]	UBP86	exp.[c]	PED (%)[d]	approximate description
a_g	ν_1	1611	1610	1534	C═O (65), C═C (14)	C═O stretch
	ν_2	1535	1511	1586	C═C (61), C═O (16)	C═C stretch
	ν_3	1301	1285	1306	C−F (56), C−C (30)	C−F stretch
	ν_4	535	532	539	C−C (62), C−F (23)	ring breath
	ν_5	415	413	418	δCCC (74)	ring bend
	ν_6	275	260	270	δCCF (88)	C−F bend
b_{3g}	ν_{23}	1485	1424		C−C (53), C−F (26)	C−C stretch
	ν_{24}	1125	1116		C−F (59), C−C (21)	C−F stretch
	ν_{25}	782	773		δCCF (49), δCCO (31)	C−F + C═O bend
	ν_{26}	400	391		δCCC (66), δCCF (20)	ring bend
	ν_{27}	275	261		δCCF (38), δCCO (45)	C−F + C═O bend
b_{1u}	ν_{10}	1438	1582		C═O (89)	C═O stretch
	ν_{11}	1068	1367		C−F (55), C−C (27), δCCC (11)	C−F stretch
	ν_{12}	907	1045		C−C (45), C−F (17), δCCF (17)	C−C stretch
	ν_{13}	508	591		δCCC (62), C−F (24)	ring bend
	ν_{14}	313	312		δCCF (85)	C−F bend
b_{2u}	ν_{18}	1707	1313		C═C (87)	C═C stretch
	ν_{19}	1189	1005		C−C (54), C−F (32)	C−C stretch
	ν_{20}	985	645		C−F (46), C−C (14), δCCF (18)	C−F stretch
	ν_{21}	315	312		δCCO (63), δCCF (27)	C═O bend
	ν_{22}	291	265		δCCF (83)	C−F bend

[a] δ bending. [b] UHF values are uniformly scaled by 0.89. [c] Experimental values in chloroform solution. [d] Calculated using UBP86/6-31G(d) force field.

TABLE 4: Vibrational Frequencies[a], PEDs and Approximate Descriptions for the In-plane normal Modes of Fluoranil Triplet (T_2) State

		frequency (cm^{-1})				
sym.	species	UHF[b]	UBP86	exp.[c]	PED (%)[d]	approximate description
a_g	ν_1	1542	1478	1543	C═O (69), C═C (14)	C═O stretch
	ν_2	1703	1653	1603	C═C (71), C═O (12)	C═C stretch
	ν_3	1235	1243	1299	C−F (54), C−C (34)	C−F stretch
	ν_4	546	554	543	C−C (66), C−F (18)	ring breath
	ν_5	414	415	419	δCCC (77)	ring bend
	ν_6	255	249	270	δCCF (82)	C−F bend
b_{3g}	ν_{23}	1397	1378		C−C (51), C−F (28)	C−C stretch
	ν_{24}	1140	1146		C−F (58), C−C (18)	C−F stretch
	ν_{25}	752	746		δCCF (44), δCCO (32)	C−F + C═O bend
	ν_{26}	408	408		δCCC (58), δCCF (21)	ring bend
	ν_{27}	281	270		δCCF (36), δCCO (51)	C−F + C═O bend
b_{1u}	ν_{10}	1567	1363		C═O (87)	C═O stretch
	ν_{11}	1328	1324		C−F (51), C−C (29), δCCC (14)	C−F stretch
	ν_{12}	1038	1039		C−C (49), C−F (18), δCCF (17)	C−C stretch
	ν_{13}	558	576		δCCC (64), C−F (21)	ring bend
	ν_{14}	302	300		δCCF (82)	C−F bend
b_{2u}	ν_{18}	1616	1582		C═C (91)	C═C stretch
	ν_{19}	1120	1241		C−C (64), C−F (24)	C−C stretch
	ν_{20}	950	974		C−F (49), C−C (20), δCCF (12)	C−F stretch
	ν_{21}	328	318		δCCO (59), δCCF (31)	C═O bend
	ν_{22}	269	261		δCCF (84)	C−F bend

[a] δ bending. [b] UHF values are uniformly scaled by 0.89. [c] Experimental values in acetonitrile solution. [d] Calculated using UBP86/6-31G(d) force field.

combination band of ring breathing and C−C−C bend (539 + 418 cm^{-1}).

3. Triplet State T_2. As discussed earlier, in polar solvents like acetonitrile, the lowest triplet excited state is likely to be the $n\pi^*$ state, and therefore, we compare the experimental data in acetonitrile to T_2 state. The symmetries, frequencies, PEDs, and approximate descriptions for the in-plane normal modes of FA triplet (T_2) obtained using UHF and UBP86 methods along with the experimental frequencies are listed in Table 4. As seen from the table, the frequencies of a_g and b_{3g} modes obtained at the UHF level (values are scaled by 0.89) are comparable to those obtained using the UBP86 method. However, there are considerable discrepancies seen for ungerade normal modes. The most intense band observed in acetonitrile at 1603 cm^{-1} can be assigned to the totally symmetric (a_g) C═C stretching fundamental. The calculated values for this normal mode is found to be at 1703 cm^{-1} (UHF) and 1653 cm^{-1} (UBP86). The only other fundamental which is observable in this region is the C═O stretching mode. However, as seen for the T_1 triplet excited state of BQ and related compounds,[64−66] the relative intensity considerations also support the assignment of this band to the C═C stretching fundamental. The relatively weaker RR band observed at 1543 cm^{-1} can be assigned to the totally symmetric C═O stretching (a_g) fundamental vibrational mode. Further, the relative shifts expected for the C═C and C═O frequencies for $n-\pi^*$ triplet excited state confirms this assignment. The band observed at 1299 cm^{-1} can be assigned to the C−F stretching (a_g) fundamental. Similarly, the RR bands

TABLE 5: Vibrational Frequencies,[a] PEDs, and Approximate Descriptions for the In-plane normal Modes of Fluoranil Radical Anion

		frequency (cm^{-1})				
sym.	species	UHF[b]	UBP86	exp.[c]	PED (%)[d]	approximate description
a_g	ν_1	1554	1546	1556	C═O (69), C═C (18)	C═O stretch
	ν_2	1682	1626	1659	C═C (64), C═O (21)	C═C stretch
	ν_3	1223	1216		C−F (66), C−C (18)	C−F stretch
	ν_4	542	540		C−C (71), C−F (12)	ring breath
	ν_5	420	420		δCCC (81)	ring bend
	ν_6	268	255		δCCF (76)	C−F bend
b_{1u}	ν_{10}	1490	1535	1502	C═O (85)	C═O stretch
	ν_{11}	1294	1285	1276	C−F (54), C−C (20), δCCC (17)	C−F stretch
	ν_{12}	1026	1022	1032	C−C (41), C−F (25), δCCF (20)	C−C stretch
	ν_{13}	565	587	565	δCCC (63), C−F (24)	ring bend
	ν_{14}	302	301		δCCF (73)	C−F bend
	ν_{18}	1565	1535	1647	C═C (87)	C═C stretch
b_{2u}	ν_{19}	1128	1208	1205	C−C (67), C−F (21)	C−C stretch
	ν_{20}	946	950	991	C−F (62), C−C (14), δCCO (13)	C−F stretch
	ν_{21}	336	327		δCCO (78), δCCF (11)	C═O bend
	ν_{22}	284	269		δCCF (85)	C−F bend

[a] δ bending. [b] UHF values are uniformly scaled by 0.89. [c] Experimental values a_g modes are obtained from RR and b_{1u} and b_{2u} from FTIR spectra. [d] Calculated using UBP86/6-31G(d) force field.

observed at 543, 419, and 270 cm^{-1} can be assigned to the a_g fundamentals of ring breath, ring bend, and C−F bend, respectively. As seen from Table, the calculated vibrational frequencies using both UHF and UBP86 methods are in good agreement with the experimental values execpt for the ν_1 and ν_2 frequencies.

The other experimentally observed bands in the lower frequency region are weak compared to the bands observed in $CHCl_3$. However, the band observed in acetonitrile at 1108 cm^{-1} is assigned to a $2 \times 419 + 270$ cm^{-1} combination band. The remaining bands are assigned to various overtone and combination bands. The band at 958 cm^{-1} is assigned to a combination band of ring breathing and C−C−C bending ($543 + 419$ cm^{-1}) mode, and the band at 1087 cm^{-1} is assigned to the first overtone of 543 cm^{-1} band. The band observed at 1240 cm^{-1} is assigned to the second overtone of 419 cm^{-1}.

4. Radical Anion. The symmetries, frequencies, PEDs, and approximate descriptions for the in-plane normal modes of FA radical anion using UHF and UBP86 methods are listed in Table 5. The resonance Raman and IR frequencies observed for the radical anion of FA are also included in the table. The frequencies calculated at UHF level (after scaling with the empirical factor of 0.89) are found to be comparable to those obtained using the UBP86 method. The approximate mode assignments given in the table are based on the PEDs calculated using the UBP86/6-31G(d) force field. The RR bands observed at 1659 and 1556 cm^{-1} can be assigned to the totally symmetric (a_g) C═C and C═O stretching fundamentals, respectively. The corresponding values calculated using both UHF (1682 and 1554 cm^{-1}) and UBP86 (1626 and 1546 cm^{-1}) methods show good agreement with the experimental results. These results are consistent with the resonance Raman study of the radical anion using pulse radiolysis method by Tripathi and Schuler.[21] Very recently, Boesch and Wheeler[40] have reported the frequencies at 1716 and 1627 cm^{-1} for C═C and C═O stretching modes, respectively, using B3P86/6-31G(d) method. This result suggests that the frequency values obtained from BP86 method compares better with the experimental data than the B3P86 method. The observation of higher value for the C═C stretching frequency compared to the C═O stretching frequency is consistent with the trend seen in the corresponding bond distances and bond orders as discussed earlier. A comparison of the calculated nontotally symmetric modes with the experimentally observed IR bands are made since these modes are expected to be active in IR. The calculated nontotally symmetric frequencies of both C═C (b_{2u}) and C═O (b_{1u}) stretching modes are obtained at the same position, i.e., at 1535 cm^{-1} from UBP86 method, whereas UHF method predicts at 1565 and 1490 cm^{-1}, respectively. The corresponding values obtained from the IR spectrum are at 1647 and 1502 cm^{-1}, respectively. The bands observed in IR spectrum at 1276 and 991 cm^{-1} are assigned to the nontotally symmetric (b_{1u} and b_{2u}) C−F stretching modes based on the calculated bands from UBP86 at 1285 and 950 cm^{-1} and at 1294 and 946 cm^{-1} from UHF method, respectively. The nontotally symmetric C−C bands calculated (UBP86) at 1022 (b_{1u}) and 1208 (b_{2u}) cm^{-1} are identified as 1032 and 1205 cm^{-1}, respectively, in the experimentally observed IR spectrum. The corresponding UHF values are at 1026 and 1128 cm^{-1}. The IR band observed at 565 cm^{-1} could be assigned to an nontotally symmetric ring bend. Both UHF and UBP86 methods are found to reproduce the experimental data with resonable accuracy.

TABLE 6: Vibrational Frequencies[a] and Approximate Descriptions for the In-Plane Normal Modes of Fluoranil Ketyl Radical ($FAH^{\bullet}$)

frequency (cm^{-1})				
UHF[b]	UBP86	exp.[c]	PED (%)[d]	approximate description
3570	3480		O−H (99)	OH stretch
1519	1620	1645	C_2-C_3 (23), C_5-C_6 (34)	CC stretch
1503	1553	1561	C_2-C_3 (37), C_1-C_6 (20), δCOH (21)	CC stretch + COH bend
1451	1490		C_5-C_6 (31), C_1-C_6 (23), δCOH (16)	CC stretch + COH bend
1437	1447	1418	C_1-C_2 (40), δCCC (21)	CC stretch
1331	1425	1348	C_4-O_2 (65), C_4-C_5 (15)	CO stretch
1300	1311			CF stretch

[a] δ bending. [b] UHF values are uniformly scaled by 0.89. [c] Experimental values in chloroform solution. [d] Calculated using UBP86/6-31G force field.

5. Ketyl Radical. The symmetries, frequencies, and approximate descriptions for the in-plane normal modes of the ketyl radical obtained at UHF/6-31G and UBP86/6-31G levels are given in Table 6. along with the experimental frequencies observed for this transient in chloroform solution. As can be seen from the table, the frequencies calculated using the UHF methods are underestimated compared to those obtained using the UBP86 method. The RR bands observed for this transient species in chloroform solution are at 1645, 1561, 1418, and 1348 cm^{-1}. The UBP86 calculation results in three modes at

TABLE 7: Comparison of the T_1 and T_2 Vibrational Frequencies (cm^{-1}) Obtained from Experimetal[a] and Theoretical[b] Results

vibl.	S_0 (^1A_G)		T_1 ($^3B_{1G}$)		$\Delta\nu_{S0-T1}$		T_2 ($^3B_{3G}$)		$\Delta\nu_{S0-T2}$	
mode	cal.	exp.	cal.	exp.	cal.	exp.	cal.	exp.	cal.	exp.
$\nu_{C=O}$	1701	1700	1610	1586	91	114	1478	1543	223	157
$\nu_{C=C}$	1678	−	1511	1534	167	−	1653	1603	25	−
ν_{C-F}	1238	1240	1285	1306	−47	−66	1243	1299	−5	−61
ν_{C-C}	528	540	532	539	−4	1	554	543	−26	−4

[a] From TR3 data; see the text for detail. [b] From the UBP86/6-31G(d) method.

1620, 1553, and 1490 cm^{-1}, with significant contribution from the C═C stretching mode. The mode with significant C═O stretching contribution is at 1425 cm^{-1}. The RR band observed at 1645 cm^{-1} can be assigned to C═C stretching fundamental. The calculated value of 1620 cm^{-1} (UBP86) compares well with this experimental frequency. The corresponding transient species of BQ[66] was shown to have its C═C stretching frequency at 1613 cm^{-1}. However, assignment of the other three bands is found to be less straightforward. A tentative assignment based on the PEDs of these bands can be given as follows: the band observed at 1561 cm^{-1} to C═C stretch + COH bend mode; the 1418 cm^{-1} band to C═C stretching mode and 1348 cm^{-1} band to the C═O stretching mode. These assignments are summarized in Table 6.

E. Structure of the T_1 Versus the T_2 State. First, we consider the characteristics of the π orbital, which is involved in $\pi\pi^*$ transition in detail. From the MO (see Figure 9b), we can see that in addition to the ring C atoms, the F atoms also have a considerable MO coefficient value which is of antibonding nature for the C−F bond. However, in the case of π^* orbital (Figure 9a), the C−F bond is of bonding character. Therefore, one would expect that there should be an increase in C−F stretching frequency on excitation. The stretching frequencies of CO/CC/CF and their differences between ground and the triplet excited states of FA are summarized in Table 7. The calculated upshift (from the ground state to the triplet excited state) in C−F stretching frequency of 47 cm^{-1} is consistent with this prediction. The corresponding experimental shift is 66 cm^{-1}. Similar comparison for the $n\pi^*$ excitation predicts that the corresponding shift will be lower than that in $\pi\pi^*$ state. This is because, in the case of n orbital, the F atoms do not have considerable MO coefficients. Thus, the calculated upshift in C−F stretching for $n\pi^*$ is 5 cm^{-1} less than that of $\pi\pi^*$. The corresponding $n\pi^*$ triplet excited-state experimental frequency shift is 61 cm^{-1}, which is 5 cm^{-1} less than that observed (66 cm^{-1}) for the $\pi\pi^*$ transition.

Similarly, the MO coefficient of ring "C" atoms for π and n orbitals suggest that there should be a larger change in its stretching frequency upon $\pi\pi^*$ excitation than in $n\pi^*$ excitation. From Figure 9, one can see that the C═C bond changes from bonding to antibonding character for $\pi\pi^*$ excitation, whereas on $n\pi^*$ excitation, the change is from nonbonding to antibonding character. The calculated frequency downshifts in the C═C stretching mode, 167 and 25 cm^{-1} for the T_1 and T_2 states, respectively, are also consistent with the above consideration. For the sake of completeness, the changes in the C═O and C−C frequencies are also included in Table. Such comparisons for C═O and C−C modes are expected to yield more or less similar results for the two excitations since in both, i.e., n and π orbitals (see Figure 9), these bonds are of nonbonding character.

All these together, support the argument of different triplet excited states of FA, in polar and nonpolar media, i.e., the $n\pi^*$ state in acetonitrile and the $\pi\pi^*$ state in $CHCl_3$. However, the limitations of the above analyses are as follows. The calculated results do not account for any solvation effect and we have considered only the pure electronic states. But in reality, it may be that the lowest triplet state may have mixed character of n and π obitals. The above calculated results can therefore be considered as an ideal case, and these predictions are upper and lower limits of the extent of the solvent effect on the structure of the triplet FA excited states.

IV. Summary

We have unequivocally identified the various transient intermediates of FA, such as ketyl radical, radical anion, and triplet excited states from our TR3 study. The vibrational frequency assignments have been carried out on the basis of comparison with ground state and related BQ intermediates. Extensive theoretical calculations using ab initio and density-functional calculations combined with normal coordinate analyses have been used to confirm the assignments of the individual bands. The calculated vibrational spectra suggests that the Hartree−Fock (UHF/6-31G(d)) method is found to slightly overestimate some of the frequencies whereas density functional method (UBP86/6-31G(d)) slightly underestimates them, but the latter is closer to the experimental data. Perfluoro effect is found to be more pronounced in the triplet excited state than in the ground state or the radical anion, whereas the effect in ground state seems to be higher than that in the radical anion. The observed differences of TR3 spectra of triplet FA in polar and nonpolar solvents are attributed to the different nature of the electronic states, i.e., $n\pi^*$ and $\pi\pi^*$, respectively.

Acknowledgment. We thank Prof. J. Chandrasekhar for helpful discussions. We thank the Jawaharlal Nehru Center for Advanced Scientific Research (JNCASR), the Department of Science and Technology (DST), and the Council of Scientific and Industrial Research (CSIR) for financial support. S.U. would like to thank DST for the award of the Swarna Jayathi Fellowship.

References and Notes

(1) Silvester, M. J. *Chem. Br*. **1993**, 215.
(2) Meyer, M.; Hagan, D. O. *Chem. Br*. **1992**, 785.
(3) Dolbier, W. R., Jr. *Chem. Rev*. **1996**, *96*, 1557 (special issue on Organofluorine Chemistry).
(4) Banks, R. E. *Organofluorine Compounds and Their Industrial Applications*; Ellis Harwood: Chichester, U.K., 1979.
(5) Banks, R. E. *Preparation, Properties and Industrial Applications of Organofluorine Compounds*; Ellis Harwood: Chichester, U.K., 1982.
(6) Atkins, P. W. *Physical Chemistry*, 3rd ed.; W. H. Freeman and Company: New York, 1985.
(7) Brahms, D. L. S.; William, P. D. *Chem. Rev*. **1996**, *96*, 1585.
(8) Yudin, A. K.; Prakash, G. K. S.; Deffieux, D.; Bradley; Bau. R.; Olah, G. A. *J. Am. Chem. Soc*. **1997**, *119*, 1572.
(9) Clouthier, D. J.; Joo, D. L. *J. Chem. Phys*. **1997**, *106*, 7479.
(10) LeGarrec, J. L.; Sidko, O.; Queffelec, J. L.; Hamon, S.; Mitchell, J. B. A.; Rowe, B. R. *J. Chem. Phys*. **1997**, *107*, 54.
(11) Asher, R. L.; Appelman, E. H.; Tilson, J. L.; Litorja, M.; Berkowitz, J.; Ruscic, B. *J. Chem. Phys*. **1997**, *106*, 9111.
(12) Harvey, J. N.; Schroder, D.; Koch, W.; Danovich, D.; Shaik, S.; Schwatz, H. *Chem. Phys. Lett*. **1997**, *273*, 164.
(13) King, R. A.; Pettigrew, N. D.; Schaefer, H. F., III *J. Chem. Phys*. **1997**, *107*, 8536.
(14) Roszak, S.; Koski, W. S.; Kaufman, J. J.; Balasubramanian, K. *J. Chem. Phys*. **1997**, *106*, 7709.
(15) Bassi, D.; Corbo, C.; Lubich, L.; Oss, S.; Scotoni, M. *J. Chem. Phys*. **1997**, *107*, 1106.
(16) Finch, C. D.; Parthasarathy, R.; Akpati, H. C.; Nordlander, P.; Dunning, F. B. *J. Chem. Phys*. **1997**, *106*, 9594.
(17) Cheng, B. M.; Preses, J. M.; Grover, J. R. *J. Chem. Phys*. **1997**, *106*, 6698.
(18) Bigelow, R. W. *J. Chem. Phys*. **1978**, *68*, 5086.

(19) Shoute, L. C. T.; Mittal, J. P. *J. Phys. Chem.* **1994**, *98*, 11094 and references therein.
(20) Darmanyan, A. P.; Foote, C. S. *J. Phys. Chem.* **1992**, *96*, 3723, 6317.
(21) Tripathi, G. N. R.; Schuler, R. H. *J. Phys. Chem*. **1983**, *87*, 3101.
(22) Schei, H.; Hagen, K.; Traetteberg, M. *J. Mol. Struct*. **1980**, *62*, 121.
(23) Meresse, P. A.; Chanh, N. B. *Acta Crystallogr*. **1974**, *B30*, 524.
(24) Girlando, A.; Pecile, C. *J. Chem. Soc., Faraday Trans. 2* **1975**, *71*, 689.
(25) Shcheglova, N. A.; Shigorin, D. N.; Yakobson, G. G.; Tsuhishvili, L. Sh. *Russ. J. Phys. Chem.* **1969**, *43*, 1112.
(26) Brundel, C. A.; Robin, M. B.; Kuebler, N. A. *J. Am. Chem. Soc.* **1972**, *94*, 1466.
(27) Chowdhury, S.; Grimsrud, E. P.; Heinis, T.; Kebarle, P. *J. Am. Chem. Soc.* **1986**, *108*, 3635.
(28) Cooper, C. D.; Frey, W. F.; Compton, R. N. *J. Chem. Phys*. **1978**, *69*, 2367.
(29) Grampp, G.; Neubauer, K. *J. Chem. Soc., Perkin Trans. 2* **1993**, 2015.
(30) Tanaka, M. *Bull. Chem. Soc. Jpn.* **1993**, *66*, 3171.
(31) Kang, E. T.; Neoh, K. G.; Tan, K. L. *Mol. Phys*. **1990**, *70*, 1057.
(32) Mourad, E. A. *Spectrochim. Acta* **1987**, *43A*, 11.
(33) Andrews, L. J.; Keefer, R. M. *J. Org. Chem*. **1988**, *53*, 537, 2163.
(34) Dodson, B.; Foster, R.; Bright, A. A. S. *J. Chem. Soc. B* **1971**, 1283.
(35) Bright, A. A. S.; Chudek, J. A.; Foster, R. *J. Chem. Soc., Perkin Trans. 2* **1975**, 1256.
(36) Boesch, S. E.; Wheeler, R. A. *J. Phys. Chem*. **1995**, *99*, 8125.
(37) Nonella, M.; Tavan, P. *Chem. Phys*. **1995**, *199*, 19.
(38) El-Azhary, A. A.; Suter, H. U. *J. Phys. Chem*. **1996**, *100*, 15056.
(39) Burie, J. R.; Boullais, C.; Nonella, M.; Mioskowksi, C.; Nabedryk, E.; Breton, J. *J. Phys. Chem. B* **1997**, *101*, 6607.
(40) Boesch, S. E.; Wheeler, R. A. *J. Phys. Chem. A* **1997**, *101*, 5799, 8351.
(41) Grafton, A. K.; Wheeler, R. A. *J. Phys. Chem. A* **1997**, *101*, 7154.
(42) Grafton, A. K.; Boesch, E. S.; Wheeler, R. A. *J. Mol. Struct. (THEOCHEM)* **1997**, *392*, 1.
(43) Mohandas, P.; Umapathy, S. *J. Phys. Chem. A* **1997**, *101*, 4449 and references therein.
(44) Qin, Y.; Wheeler, R. A. *J. Phys. Chem*. **1997**, *100*, 10554.
(45) Keszthelyi, T.; Wilbrandt, R.; Bally, T. *J. Phys. Chem*. **1996**, *100*, 16843.
(46) Keszthelyi, T.; Wilbrandt, R.; Bally, T.; Roulin, J. L. *J. Phys. Chem*. **1996**, *100*, 16850.
(47) Balakrishnan, G.; Mohandas, P.; Umapathy, S. *J. Phys. Chem*. **1996**, *100*, 16472.
(48) Balakrishnan, G.; Umapathy, S. *J. Chem. Soc., Faraday Trans*. **1997**, *93*, 4125.
(49) Myers, A. B.; Mathies, R. A. In *Biological Applications of Raman Spectroscopy*; Spiro, T. G., Ed.; Wiley: New York; Vol. 2, 1987, p 1.
(50) Biswas, N.; Umapathy, S.; Kalyanaraman, C.; Sathyamurthy, N. *Proc. Ind. Acad. Sci. (Chem. Sci.)* **1995**, *107*, 233.
(51) Albrecht, A. C. *J. Chem. Phys*. **1961**, *34*, 1476.
(52) Torrey, H. A.; Hunter, W. H. *J. Am. Chem. Soc*. **1912**, *34*, 708.
(53) Frisch, M. J.; Trucks, G. W.; Schlegel, H. B.; Gill, P. M. W.; Johnson, B. G.; Robb, M. A.; Cheeseman, J. R.; Keith, T.; Petersson, G. A.; Montgomery, J. A.; Raghavachari, K.; Al-Laham, M. A.; Zakrzewski, V. G.; Ortiz, J. V.; Foresman, J. B.; Cioslowsski, J.; Stefanov, B. B.; Nanayakkara, A.; Challacombe, M.; Peng, C. Y.; Ayala, P. Y.; Chen, W.; Wong, M. W.; Andres, J. L.; Replogle, E. S.; Gomperts, R.; Martin, R. L.; Fox, D. J.; Binkley, J. S.; Defrees, D. J.; Baker, J.; Stewart, J. P.; Head-Gordon, M.; Gonzalez, C.; Pople, J. A. *Gaussian 94*, Revision C.2. Gaussian, Inc., Pittsburgh, PA, 1995.
(54) Becke, A. D. *Phys. Rev. A* **1988**, *38*, 3098.
(55) Perdew, J. P. *Phys. Rev. B* **1986**, *33*, 8822.
(56) Hohenberg, P.; Khon, W. *Phys. Rev. B* **1964**, *136*, 864.
(57) Kohn, W.; Sham. L. J. *Phys. Rev. A* **1965**, *140*, 1133.
(58) Slater, J. C. *Quantum Theory of Molecules and Solid*: *The Self-Consistent Field for Molecules and Solids*; McGraw-Hill: New York, 1974; Vol. 4.
(59) Schlegel, H. B. *J. Comput. Chem*. **1982**, *3*, 214.
(60) Sundius, T. *MOLVIB, Calculation of Harmonic Force Fields and Vibrational Modes of Molecule*, QCPE # QCMP 103; University of Helsinki: Helsinki, Finland, 1991 (downloadable from http://qcpe.chem.indiana.edu).
(61) Schlegel, H. B.; Krishnan, R.; Defrees, D. J.; Binkely, J. S.; Frisch, M. J.; Whiteside, R. A.; Hout, R. F.; Hehre, W. J. *Int. J. Quantum Chem.* **1989**, *S15*, 269.
(62) Hubig, S. M.; Bockman, T. M.; Kochi, J. K. *J. Am. Chem. Soc*. **1997**, *119*, 2926.
(63) Nakano, T.; Mori, Y. *Bull. Chem. Soc. Jpn*. **1994**, *67*, 2627.
(64) Rossetti, R.; Beck, S. M.; Brus, L. E. *J. Phys. Chem*. **1983**, *87*, 3058.
(65) Tahara, T.; Hamaguchi. T. *J. Phys. Chem*. **1992**, *96*, 8252.
(66) Tripathi, G. N. R.; Schuler,R. H. *J. Phys. Chem*. **1987**, *91*, 5881.